ELSEVIER

Journal of Alloys and Compounds 356–357 (2003) 137–141

Journal of ALLOYS AND COMPOUNDS

www.elsevier.com/locate/jallcom

Electron density-of-states and the metal–insulator transition in LaH_x

R.G. Barnes[a,*], C.T. Chang[a,b], G. Majer[c], U. Kaess[c,d]

[a]*Department of Physics and Ames Laboratory, USDOE, Iowa State University, Ames, IA 50011, USA*
[b]*Millennium Technology, Inc., 465-5600 Parkwood Way, Richmond, BC, Canada V6V 2M2*
[c]*Max-Planck-Institut für Metallforschung, Heisenbergstrasse 1, 70569 Stuttgart, Germany*
[d]*Robert Bosch GmbH, Automotive Electronics, AE/SPP5, Tübinger Strasse 123, 72762 Reutlingen, Germany*

Received 10 June 2002; accepted 26 October 2002

Abstract

The temperature dependence of the Gd^{3+} impurity ion spin relaxation rate, τ_i^{-1}, in lanthanum hydrides, LaH_x ($2.0 \leq x \leq 3.0$), probes the metal–insulator (MI) transition in this system. Because Gd^{3+} is an S-state ion, τ_i^{-1} depends on interaction with conduction electrons in the metallic state, resulting in Korringa-type behavior, $\tau_i T =$ constant, and $(\tau_i T)^{-1/2} \propto N(E_F)$, the electronic density-of-states at the Fermi level. In the non-metallic state, weak phonon processes result in a temperature dependence, $\tau_i^{-1} \propto T^n$, with $3 < n < 5$. The rate τ_i^{-1} has been measured via the Gd^{3+}-induced contribution, R_{1p}, to the proton spin-lattice relaxation rate, R_1, by comparing the measured rate in pure LaH_x with that in LaH_x containing controlled low levels of Gd. The results show that in the metallic state, $N(E_F) \propto (2.91 - x)^{1/3}$, consistent with earlier results based on the ^{139}La Knight shift which also support $N(E_F) \propto (2.91 - x)^{1/3}$.

Keywords: Metal–insulator transition; Lanthanum hydrides: electronic structure

1. Introduction

Previous NMR studies have traced the x-dependence of the electronic density-of-states (DOS) at the La sites in LaH_x ($2.0 \leq x \leq 3.0$) at temperatures above the metal–insulator (MI) and order–disorder (OD) transitions, i.e. at $T > 250$ K, via the ^{139}La Knight shift, $K(^{139}La)$, and at the hydrogen sites at temperatures below these transitions, i.e. at $T < 250$ K, via the conduction electron contribution R_{1e} to the proton spin-lattice relaxation rate, R_1 [1,2]. These measurements are consistent with the DOS following nearly-free-electron-like behavior, i.e. decreasing approximately as $(3 - x)^{1/3}$, as expected if the conduction electron density decreases linearly with increasing x. On the other hand, low-temperature measurements ($T < 8$ K) of the x-dependence of the specific heat parameter γ are consistent with the DOS decreasing approximately as $(3 - x)$ [3]. A further magnetic resonance approach to probing the DOS and the MI transition is to measure the temperature dependence of the spin-lattice relaxation rate, τ_i^{-1}, of Gd^{3+} impurity ions in LaH_x. Because Gd^{3+} is an S-state ion, τ_i^{-1} depends on interaction with conduction electrons in the metallic state, resulting in Korringa-type behavior, $\tau_i T =$ constant, and $(\tau_i T)^{-1/2} \propto N(E_F)$, the DOS at the Fermi level as modified by the Stoner factor which includes exchange and correlation enhancement effects. In the nonmetallic state, phonon processes yield the temperature dependence, $\tau_i^{-1} \propto T^n$, with $3 < n < 5$. The rate τ_i^{-1} has been measured at temperatures and compositions (x-values) both below and above the MI transition via the Gd^{3+}-induced contribution to the proton spin-lattice relaxation rate, R_1, by comparing the measured rate in LaH_x containing controlled low levels, e.g. 25–300 ppm, of Gd with that in pure LaH_x.

2. Theoretical background

The proton spin-lattice relaxation rate, R_1, in metal–hydrogen systems frequently results from three contributions [4],

$$R_1 = R_{1d} + R_{1e} + R_{1p} \quad (1)$$

Here, R_{1d} is the proton–proton dipolar relaxation rate; R_{1e} results from the coupling of the proton moment to the conduction electrons (the Korringa rate), and R_{1p} arises from the dipolar coupling between the proton moment and

*Corresponding author.
E-mail address: barnes@ameslab.gov (R.G. Barnes).

0925-8388/02/$ – see front matter
doi:10.1016/S0925-8388(02)01221-5

the fluctuating electronic moment of paramagnetic impurity ions.

The strength of the proton–impurity moment interaction is defined by $\tau^{-1}(r) = Cr^{-6}$ where $\tau^{-1}(r)$ is the relaxation rate that a single proton would have at a distance r from the ion. For powder samples, C is given by [5,6]

$$C = (2/5)(\gamma_p\gamma_n\hbar)^2\, J(J+1)\,[\tau_i/(1+\omega_o^2\tau_i^2) + 7\tau_i/3(1+\omega_e^2\tau_i^2)] \quad (2)$$

where J, γ_p, τ_i, and ω_e are the angular momentum, gyromagnetic ratio, spin-lattice relaxation time and Larmor frequency of the ion, respectively, and γ_n and ω_o are the corresponding quantities for the proton. The relative importance of direct relaxation characterized by C and that due to diffusion characterized by D (whether spin or atom) is described by the pseudopotential radius, $\beta = (C/D)^{1/4}$, which is the distance from the impurity at which the rate of diffusion to the impurity equals the relaxation rate at the impurity. A second important parameter in the low-temperature rigid-lattice regime is the spin-diffusion barrier radius, b, which is roughly the distance at which the magnetic field due to the ion equals the local nuclear dipolar field at a proton site in the lattice, and within which spin diffusion is inhibited [5,6]. In the atom diffusion regime, b is replaced by the proton spin–ion spin nearest-neighbor spacing a_1. Finally, the relative significance of b (or a_1) and β is expressed by the parameter $\delta = \beta^2/2b^2 = (C/D)^{1/2}/2b^2$. The general form for the relaxation rate is then [5,6]

$$R_{1p} = 8\pi ND\beta[\Gamma(3/4)/\Gamma(1/4)][I_{3/4}(\delta)/I_{-3/4}(\delta)] \quad (3)$$

Here the $I_m(\delta)$ are the modified Bessel functions of fractional order, and N is the number density of impurity ions. This result applies to both spin and atom diffusion, i.e. D_s or D_a, with the limiting forms appropriate to the fast and slow diffusion regimes, i.e. weak and strong collision regimes, determined by δ. Approximately, $\delta \geq 2$ or $\beta \geq 2b$, defines the strong collision regime, and $\delta \leq 0.3$ or $\beta \leq 0.8b$ defines the weak collision regime. We focus here on the behavior of R_{1p} in the low-temperature spin-diffusion and high-temperature atom-diffusion regimes, which span the MI transition, and which are most amenable to quantitative interpretation.

3. Experimental aspects

All of the lanthanum hydride samples were prepared in the Materials Preparation Center of the Ames Laboratory from the highest purity lanthanum metal available. Details of their preparation were given previously in Ref. [2]. The pure (undoped) samples are those that were used in previous studies of the proton spin-lattice relaxation rate and ^{139}La Knight shift [2] and of hydrogen diffusivity [7]. The magnetic resonance instrumentation was also described in detail in Ref. [6]. All of the measurements reported here were made at a resonance frequency of 40 MHz.

The procedure followed has been to measure the temperature dependence of the proton R_1 in pure LaH_x and in the same composition containing a controlled low level of Gd impurity. For the low impurity levels involved, never greater than 300 ppm, there is no evidence that the R_{1d} and R_{1e} contributions in Eq. (1) differ in the two cases. Subtraction of the rate in the pure sample from that in the Gd-doped sample yields R_{1p}. The rate R_{1p} is a direct, linear function of the Gd content at least up to an impurity level of 1000 ppm.

All features of the Gd-induced spin-lattice relaxation are evident in the temperature dependence of R_{1p} for $LaH_{2.61}$: 300 ppm Gd and $LaH_{2.60}$: 25 ppm Gd shown in Fig. 1. This is the highest hydrogen concentration studied that shows unambiguous metallic character at both low and high temperatures. In addition, $LaH_{\sim 2.60}$ shows only a negligible trace of the two-phase character evident at all higher x-values, which has been attributed to the accompanying OD transition [8]. At low temperatures, in the spin-diffusion regime, R_{1p} passes through a maximum when the condition $\omega_o\tau_i \approx 1$ is satisfied. At approximately 150 K, atom diffusion becomes faster than spin diffusion, and R_{1p} increases exponentially. With further increasing temperature, R_{1p} passes through a second maximum at about 250 K when atom diffusion becomes sufficiently fast that multiple encounters with an impurity spin are required to relax the proton spin. This is the weak collision regime (fast atom diffusion regime) in which R_{1p} is independent of the atom diffusivity, D_a, but depends directly (or very nearly directly) on τ_i.

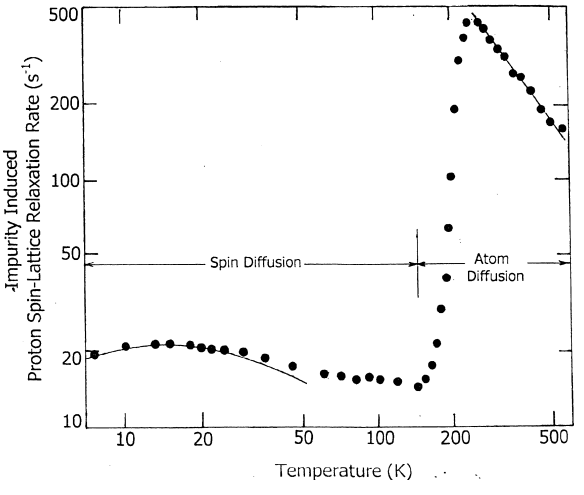

Fig. 1. Temperature dependence of the Gd-induced spin-lattice relaxation rate, R_{1p}, in metallic $LaH_{2.61}$: 300 ppm Gd ($T < 130$ K) and in metallic $LaH_{2.60}$: 25 ppm Gd ($T > 130$ K). The solid curves through the low-temperature data points and the straight line through the high-temperature points are best fit results (see text). Measurements were made at a resonance frequency of 40 MHz.

3.1. Low temperatures (spin diffusion regime)

As noted above, in this limit for spin diffusion, an important feature results when $\omega_o\tau_i \approx 1$, which maximizes the first term in brackets in C [Eq. (2)], which enters Eq. (3) via the pseudo-potential radius β. The second term in brackets is negligible since $(\omega_e\tau_i)^2 \gg 1$. This condition creates a 'peak' in the temperature dependence of R_{1p}. The analysis is complicated, however, by the barrier radius b which also depends on τ_i and by the parameter δ which depends on τ_i via both b and C. Assuming that $\tau_i^{-1} \propto T^n$, the low-temperature behavior can be fit to determine n. The solid curve through the low-temperature data points in Fig. 1 shows the fit with $\tau_i^{-1} \propto T^{1.00}$ for $LaH_{2.60}$: 300 ppm Gd.

3.2. High temperatures (atom diffusion regime)

With increasing temperature, the atom diffusion rate exceeds that due to spin diffusion, and since the activation enthalpy, H_a, for hydrogen diffusion decreases rapidly with increasing x [7], the high-temperature R_{1p} maximum shifts progressively to lower temperatures. At the same time, the maximum value of R_{1p} increases sharply as the Gd^{3+} spin relaxation rate, τ_i^{-1}, slows down with decreasing metallic character, reflecting the decreasing electron DOS. These features are evident in Fig. 2 which shows the temperature dependence of R_{1p} due to 25 ppm Gd in LaH_x, $x = 2.00$, 2.25, 2.60, and 3.00. The temperature at which the maximum occurs shifts from 500 K at $x = 2.00$ to 250 K at $x = 2.60$ and 3.00, and the maximum R_{1p} increases by a factor of 80 between $x = 2.00$ and $x = 3.00$—indeed, by a factor of ~18 between 2.60 and 3.00. Fig. 2 also shows, for $x = 3.00$, the temperature range in which two proton resonances occur in both the pure and Gd-doped samples. These have been identified as arising from the ordered (low-temperature) and disordered (high-temperature) phases [8], and appear for $x \geq 2.70$.

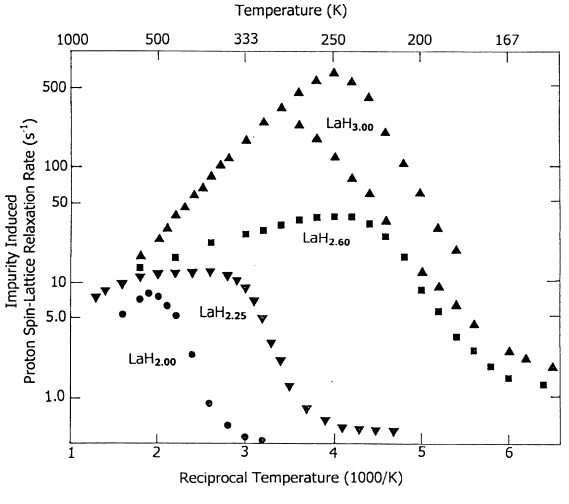

Fig. 2. Temperature dependence of the Gd-induced rate R_{1p} in LaH_x, $x = 2.00$, 2.25, 2.60, and 3.00, in the atom-diffusion regime. The rates shown have been standardized to an impurity concentration N of 25 ppm, based on the experimentally demonstrated linear dependence of R_{1p} on N. All measurements were made at a resonance frequency of 40 MHz.

In the fast atom diffusion (weak collision) limit ($\beta < a_1$), many encounters are needed to yield relaxation, and R_{1p} becomes independent of D_a. In this limit, Eq. (3) becomes [9]

$$R_{1p} = \beta_o NC/a_o^3 \quad (4)$$

Here a_o is the cubic lattice parameter, and β_o is a lattice-specific sum over impurity ion sites, i.e. $\beta_o = (64/Z)\Sigma_i \rho_i^{-6}$, where Z is the number of lattice sites per cubic cell. However, at high temperatures, the mean dwell time for diffusive hopping, τ_D, may become short enough that τ_D^{-1} becomes comparable to or greater than τ_i^{-1}. In this case, τ_i in Eq. (2) is replaced by $\tau^{*-1} = \tau_i^{-1} + \tau_D^{-1}$, and consequently reliable, independent values of τ_D and its temperature dependence are needed to obtain those of τ_i. These measurements have recently been made [7], furnishing values for the temperature dependence of the diffusivity, D_a, and of the activation enthalpy for diffusion, H_a, for LaH_x, $2.0 \leq x \leq 3.0$. Values of τ_D are obtained from the relation, $D_a = \langle L^2 \rangle / 6\tau_D$, where L is the diffusive path length, shown in recent neutron diffraction studies [10] to be the T–O site spacing, 0.244 nm, at high x-values.

Now R_{1p} is determined by Eq. (4), with $(\omega_o\tau^*)^2 \ll 1$ and $(\omega_e\tau^*)^2 \gg 1$, so that the first term in the square brackets in Eq. (2) becomes τ^* and the second term is negligible, with the result that $R_{1p} \propto \tau^*$. The temperature dependence of R_{1p} yields that of τ^*, and with knowledge of τ_D the temperature dependence of τ_i can be obtained. This is the procedure followed to analyze the high temperature measurements for x-values beginning with $x = 2.60$.

4. Results and discussion

4.1. Metallic state

Results for the metallic state, in which $\tau_i^{-1} \propto T$, are shown in Fig. 3, where the low temperature, i.e. $T < 250$ K, measurements are indicated by squares and those for $T > 250$ K, by circles. These show that LaH_x remains metallic at low temperatures at least up to and including $x = 2.80$. This is consistent with resistivity results that show a transition from metallic to semiconducting behavior at $T \approx 250$ K for $x = 2.70$, 2.80 and intermediate compositions up to 2.90 [11,12], but semiconducting only at $x = 2.93$ [11]. In the present work, measurements at $x = 2.90$ failed to detect the low-temperature R_{1p} peak, probably because, if there is one, it occurs at $T \approx 170$ K and is hidden by the sharp rise in R_{1p} when $D_a > D_s$ (Fig. 1). For $x = 2.60$, the R_{1p} measurements show metallic behavior at both low and

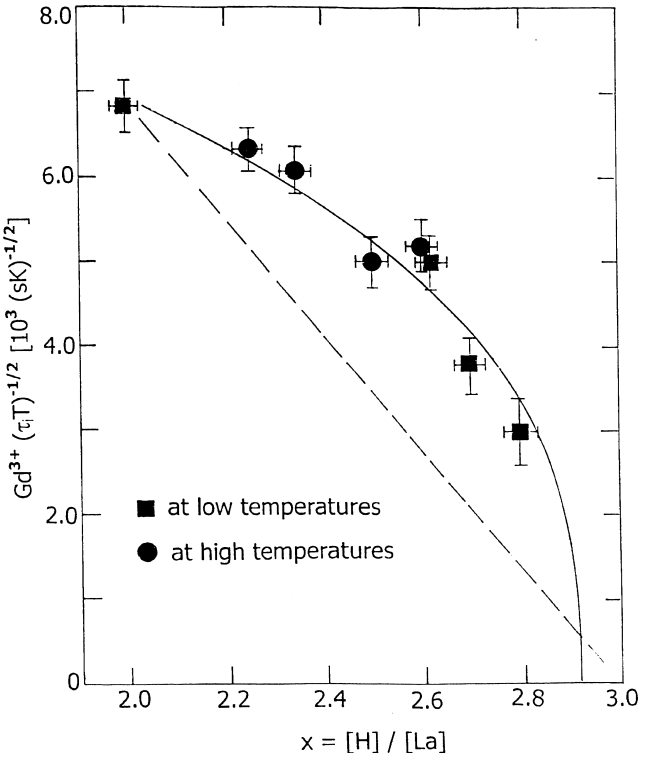

Fig. 3. Dependence of $(\tau_i T)^{-1/2}$ for Gd^{3+} on hydrogen concentration, $x=[H]/[La]$. Circles are for measurements made at high temperatures ($T>250$ K), and squares for those made at low temperatures ($T<250$ K). The solid curve is the best fit of $(\tau_i T)^{-1/2} \propto (x_c - x)^{1/3}$ to the data, with $x_c = 2.91$, and the dashed line shows $(3-x)$ behavior.

high temperatures. Therefore, we conclude that LaH_x remains metallic at all temperatures for $x \leq 2.60$, and at low temperatures for $2.60 \leq x \leq 2.80$.

The principal feature of Fig. 3 is the dependence of $(\tau_i T)^{-1/2}$ on hydrogen concentration x. The solid curve shows the least-squares fit (regression coefficient $r=0.997$) for $(\tau_i T)^{-1/2} \propto N(E_F) \propto (x_c - x)^{1/3}$, which is the dependence expected if $N(E_F)$ follows essentially rigid-band free-electron-like behavior, with the conduction electron density, n, decreasing linearly as x increases from 2 to $x_c = 2.91$, reflecting the withdrawal of electrons from the Fermi level to form a bonding band with O-site hydrogen atoms, x_c being the critical x-value. The dashed straight line in Fig. 3 shows the approximate dependence of the specific heat parameter γ on x [3]. Assuming that $\gamma \propto N(0)$, the 'bare' DOS, then these data imply $N(0) \propto (3-x)$.

As noted earlier, NMR measurements of $K(^{139}La)$ at $T>250$ K and of the proton R_{1e} at $T<250$ K are also consistent with $N(E_F) \propto (x_c - x)^{1/3}$ [1,2]. These measurements are shown in Fig. 4 (adapted from Fig. 1 of Ref. [2]). The solid curves are least-squares fits of $(x_c - x)^{1/3}$ to the data points. It is significant that the fit curve for $K(^{139}La)$ also yields $x_c = 2.91$. In making this fit, the two data points at $x=2.92$ and 2.99 have been excluded. These points show that the shift becomes constant at 0.118% at temperatures greater than 250 K, suggestive of a chemical

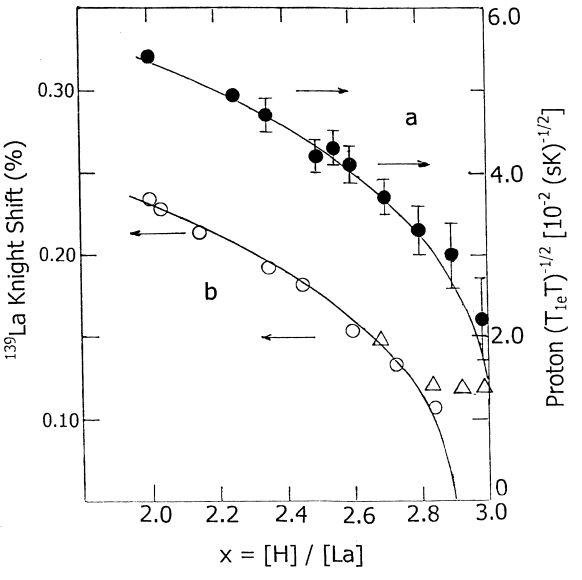

Fig. 4. Dependence of the proton $(T/R_{1e})^{-1/2} = (T_{1e}T)^{-1/2}$ (a), and of $K(^{139}La)$ (b), on hydrogen concentration, $x=[H]/[La]$, adapted from Ref. [2]. For $K(^{139}La)$ the circles are from Ref. [1], and the triangles are Ames Laboratory results. The proton $(T_{1e}T)^{-1/2}$ data are Ames Laboratory results. The solid curves through the data points are least-squares fits of $(x_c - x)^{1/3}$ with $x_c = 2.91$ for $K(^{139}La)$ and 3.04 for the proton $(T_{1e}T)^{-1/2}$.

shift in the nonmetallic phase [2]. For $T<T_{OD}$ the rapid increase in the ^{139}La resonance linewidth due to second-order quadrupole broadening poses severe difficulties to measuring the Knight shift at low temperatures [13]. The proton $(T_{1e}T)^{-1/2}$ results at high x-values may be unreliable due to the R_{1p} contribution from the residual rare-earth impurity content, even though the samples were based on the highest available purity Ames Laboratory La metal. This could account for the fact that these data yield $x_c = 3.04$.

4.2. Insulating (semiconducting) state

Following the data analysis procedure described above, and taking account of τ_D^{-1}, the high-temperature results for $x=2.70$, 2.80, 2.90, and 3.00 conform to $\tau_i^{-1} \propto T^n$ behavior with $n=3.9\pm0.5$. This is consistent with the Gd^{3+} spin relaxation rate measured in insulating solids [14], and confirms the insulating (semiconducting) character of the high-temperature disordered phase for $x \geq 2.70$.

5. Conclusions

Measurements of the temperature dependence of the Gd^{3+} spin-lattice relaxation rate in LaH_x, $2.00 \leq x \leq 3.00$, support the following conclusions:

1. LaH_x is metallic at all temperatures for $x \leq 2.60$.
2. For $2.60 \leq x \leq 2.91$, LaH_x is metallic at low tempera-

tures and insulating (semiconducting) at high temperatures.
3. For $x \geq 2.91$, LaH_x is insulating at all temperatures.
4. In the metallic state, whether at low or high temperatures, the electron DOS at the Fermi level, $N(E_F)$, follows rigid-band, free-electron-like behavior, i.e. $N(E_F) \propto (2.91 - x)^{1/3}$.

In addition, previous measurements [1,2] of $K(^{139}La)$ also support the conclusion that $N(E_F) \propto (2.91 - x)^{1/3}$ in the metallic state. The earlier $K(^{139}La)$ results also indicate that LaH_x is insulating (semiconducting) for $x \geq 2.91$, consistent with the present $(\tau_i T)^{-1/2}$ results. Moreover, although the details of the dependence of the proton R_{1e}, of $K(^{139}La)$, and of $\tau_i^{-1}(Gd^{3+})$ on $N(E_F)$ involve different effective hyperfine fields and/or exchange integrals and Stoner enhancement factors [4,15], the result is that all three NMR approaches yield essentially the same result at both low and high temperatures within the metallic state.

Acknowledgements

Ames Laboratory is operated for the U.S. Department of Energy by Iowa State University under Contract W-7405-Eng-82. This work was supported by the Director for Energy Research, Office of Basic Energy Sciences.

References

[1] D.S. Schreiber, R.M. Cotts, Phys. Rev. 131 (1963) 1118.
[2] R.G. Barnes, C.T. Chang, M. Belhoul, D.R. Torgeson, B.J. Beaudry, D.T. Peterson, J. Less-Common Met. 172–174 (1991) 411.
[3] K. Kai, K.A. Gschneidner Jr., B.J. Beaudry, D.T. Peterson, Phys. Rev. B 40 (1989) 6591.
[4] R.G. Barnes, in: H. Wipf (Ed.), Hydrogen in Metals III, Springer, Berlin, 1997, p. 93.
[5] H.E. Rohrschach Jr., Physica (Utrecht) 30 (1964) 38.
[6] T.T. Phua, B.J. Beaudry, D.T. Peterson, D.R. Torgeson, R.G. Barnes, M. Belhoul, G.A. Styles, E.F.W. Seymour, Phys. Rev. B 28 (1983) 6227.
[7] G. Majer, U. Kaess, R.G. Barnes, Phys. Rev. Lett. 83 (1999) 340.
[8] R.G. Barnes, B.J. Beaudry, D.R. Torgeson, C.T. Chang, R.B. Creel, J. Alloys Comp. 253–254 (1997) 445.
[9] E.F.W. Seymour, C.A. Sholl, J. Phys. C Solid State Phys. 18 (1985) 4521.
[10] C. Karmonik, T.J. Udovic, J.J. Rush, in: R.C. Bowman, W.B. Jackson, R.G. Leisure, N.N. Nickel (Eds.), Hydrogen in Semiconductors and Metals, Mater. Res. Soc. Symp. Proc., Vol. 513, Materials Research Society, Pittsburgh, 1998, p. 149.
[11] J. Shinar, B. Dehner, B.J. Beaudry, D.T. Peterson, Phys. Rev. B 37 (1988) 2066.
[12] J. Shinar, B. Dehner, R.G. Barnes, B.J. Beaudry, Phys. Rev. Lett. 64 (1990) 563.
[13] R.G. Barnes, B.J. Beaudry, R.B. Creel, D.R. Torgeson, D.G. de Groot, Solid State Commun. 36 (1980) 105.
[14] R. Bierig, M. Weber, S. Warshaw, Phys. Rev. 134 (1964) A1504.
[15] R.H. Taylor, Magnetic Ions in Metals, Taylor & Francis, Halstead Press, New York, 1977.